DISSIPATIVE RANGE STATISTICS OF TURBULENT FLOWS WITH VARIABLE VISCOSITY

Michael Gauding, Luminita Danaila and Émilien Varea
CORIA – CNRS UMR 6614
Université de Rouen
76801 Saint Etienne du Rouvray, France
michael.gauding@coria.fr

Abstract

The decay of homogeneous isotropic turbulence in a variable viscosity fluid is analyzed by means of highly resolved direct numerical simulations. An important question that is addressed by the present work is how the dissipation mechanism is changed by fluctuations of the viscosity. From the budget equation of the turbulent energy it is shown that the mean dissipation is nearly unchanged by variable viscosity effects. This result is explained by a negative correlation between the local viscosity and the local velocity gradients. However, the dissipation is a highly fluctuating quantity with a strong level of intermittency. From a statistical analysis it is shown that turbulent flows with variable viscosity are characterized by an enhanced level of small-scale intermittency, which results in the presence of smaller length scales and a modified turbulent mixing. The effect of variable viscosity on the turbulent cascade is analyzed by two-point statistics.

1 Introduction

Turbulent flows encountered in engineering and environmental applications are very often characterized by a spatial or temporal variation of viscosity, which results from variations of temperature or species composition. A prominent example from geophysical flows is the convection in the earth's mantle, where the viscosity decreases with temperature. An other important case is the turbulent mixing in combustion systems, where a concentration dependent viscosity may affect the efficiency of turbulent mixing.

Fully developed turbulence is characterized by a large range of length scales, varying from the so-called integral length scale l_t, at which large velocity fluctuations occur on average, down to the smallest scale, the so-called Kolmogorov or dissipation scale η, at which turbulent fluctuations are dissipated due to viscosity. According to Kolmogorov's first hypothesis (Kolmogorov (1941*b*,*a*)), the smallest scales should reveal universal properties, and should depend only on two parameters, namely the viscosity ν and the mean energy dissipation rate $\langle\varepsilon\rangle$. Kolmogorov's second hypothesis postulates that larger scales of the flow decouple from the smaller scales and should become independent of viscosity, provided that the Reynolds number is sufficiently high. However, numerous experimental and numerical studies have indicated that Kolmogorov's traditional view is a crude assumption and that large and small scale quantities are strongly coupled, cf. Sreenivasan & Antonia (1997) and Warhaft (2000). The situation is even more complex for turbulent mixing with local viscosity variations. One has to cope with a turbulence-scalar interaction which is two-fold: the fluid motions affect the scalar mixing, while mixing induced viscosity changes affect the dynamics of the velocity field.

Viscosity represents the most important property of turbulent flows, and the impact of its variation on the dynamics should be addressed in detail. Taylor (1935) postulated that the mean energy dissipation rate depends only on the large scale velocity u_{rms} and length scale l_t, i.e. $\langle\varepsilon\rangle \propto u_{\mathrm{rms}}^3/l_t$, and hence becomes independent of viscosity, provided that the Reynolds number is sufficiently large. However, the dissipation is a highly fluctuating quantity with large but rare excursions from its mean value. In the literature this phenomenon is called internal intermittency, cf. Batchelor & Townsend (1949). The physical mechanism behind internal intermittency is still unresolved, and it is not known whether viscosity gradients enhance or reduce internal intermittency. Internal intermittency is present for both the velocity and scalar fields. The consequence for turbulent mixing is evident: large fluctuations of the scalar dissipation correspond to large values of the local scalar gradient, which enhances the mixing efficiency.

The paper is structured as follows. Section 2 presents the governing equations and the direct numerical simulations on which the analysis is based. Section 3 introduces the budget equation of the turbulent energy and discusses the impact of variable viscosity on the dissipation mechanism of turbulence. Section 4 addresses the impact of variable viscosity on the Kolmogorov length scale. A two-point analysis is presented in section 5 and we conclude this study in section 6.

2 Direct numerical simulations and governing equations

The present work studies the effect of local viscosity variations on small-scale turbulence. The analysis is based on highly resolved direct numerical simulations (DNS) of decaying homogeneous isotropic turbulence. The DNS solves the three-dimensional incompressible Navier-Stokes equations,

$$\frac{\partial u_j}{\partial t} + u_i \frac{\partial u_j}{\partial x_i} = -\frac{\partial p}{\partial x_j} + \frac{\partial}{\partial x_i}\left(2\nu s_{ij}\right) , \qquad (1)$$

with the continuity equation

$$\frac{\partial u_i}{\partial x_i} = 0 , \qquad (2)$$

in a triply periodic box with size 2π by a pseudo-spectral method, see Gauding *et al.* (2015) for a detailed description of the algorithm. Einstein's summation convention is used, which implies summation over indices appearing twice. In eqs. (1) and (2), the velocity field is denoted by u_j, p is the pressure (for simplicity the density $1/\rho$ is incorporated in p), ν is the local viscosity, and s_{ij} is the strain-rate tensor, defined as

$$s_{ij} = \frac{1}{2}\left(\frac{\partial u_j}{\partial x_i} + \frac{\partial u_i}{\partial x_j}\right) . \qquad (3)$$

The local viscosity field $\nu(\boldsymbol{x}, t)$ is determined by solving an advection-diffusion equation for a scalar field $\phi(\boldsymbol{x}, t)$, i.e.

$$\frac{\partial \phi}{\partial t} + u_i \frac{\partial \phi}{\partial x_i} = D \frac{\partial^2 \phi}{\partial x_i^2} . \qquad (4)$$

The scalar ϕ is statistically isotropic and homogeneous, bounded, i.e. $-1 \leq \phi(\boldsymbol{x}, t) \leq 1$, and has zero mean, i.e. $\langle\phi\rangle = 0$. Following Gréa *et al.* (2014), the local viscosity $\nu(\boldsymbol{x}, t)$ is linked through a linear relation to the scalar field,

$$\nu(\boldsymbol{x}, t) = \langle\nu\rangle + \nu'(\boldsymbol{x}, t) = \langle\nu\rangle + c\phi(\boldsymbol{x}, t) , \qquad (5)$$

where $\langle\nu\rangle$ denotes the uniform mean viscosity, $\nu'(\boldsymbol{x}, t)$ denotes the fluctuating viscosity field, and c is a positive constant with $c < \langle\nu\rangle$ to ensure positivity of $\nu(\boldsymbol{x}, t)$. A linear relation is convenient because it keeps the mean viscosity $\langle\nu\rangle$ unchanged during decay. The constant c is obtained from the initial minimum and maximum values of the viscosity by $c = (\nu_{\max} - \nu_{\min})/2$, which implies that the initial scalar variance $\langle\phi^2\rangle$ equals unity. In the following, we use ϕ as a surrogate for ν. The molecular diffusivity D in eq. (4) is assumed to be constant and equals the mean viscosity $\langle\nu\rangle = (\nu_{\min} + \nu_{\max})/2$. As a consequence the Schmidt number, defined as $Sc = \nu/D$, is a fluctuating quantity.

The initialization of the DNS is similar to that of Ishida *et al.* (2006). The initial velocity field obeys a broad-band spectrum of the type

$$E(\kappa, t = 0) \propto \kappa^4 \exp(-2(\kappa/\kappa_p)^2) , \qquad (6)$$

where κ denotes the wave-number. The peak of the initial spectrum is located at $\kappa_p = 12$ to inject energy at sufficiently large length scale, and to keep the initial integral length scale small compared to the confinement by the computational domain. The initial scalar energy spectrum is proportional to the velocity spectrum, and the initial scalar field is not correlated with the velocity field, i.e. $\langle u_i \phi\rangle = 0$. The initialization guarantees that both velocity and scalar field are statistically homogeneous and isotropic. The initial Reynolds number, defined with the mean viscosity as $Re_0 = u_{\mathrm{rms}}/(\kappa_p\langle\nu\rangle)$, equals 43, where $u_{\mathrm{rms}} = \sqrt{\langle u_i^2\rangle/3}$ is the root mean square of the velocity field.

The governing equations are temporally integrated by a low-storage stability preserving third order Runge-Kutta method. The viscous term containing the mean viscosity $\langle\nu\rangle$ is treated exactly by an integrating factor technique. The fluctuating part of the viscous term is non-linear and computed in real space by a sixth-order compact method, cf. Lele (1992). To remove aliasing effects a standard isotropic truncation method in combination with a random phase-shift technique is employed. This allows us to keep all wave-numbers $\kappa < \sqrt{2}N/3$. The grid resolution of the DNS is $N^3 = 1024^3$, which adequately resolves the smallest scales for all cases.

In this work we will compare DNS with constant and variable viscosity. The baseline case has a constant and spatially uniform viscosity of $\langle\nu\rangle = 0.006$. Additionally, two cases with variable viscosity are considered. These cases have the same mean viscosity $\langle\nu\rangle$ as the baseline case, but an initial viscosity ratio $R_\nu = \nu_{\max}/\nu_{\min}$ that equals 5 and 15, respectively. The initial viscosity distribution is bimodal with an initial normalized viscosity variance of $\langle\nu'^2\rangle/\langle\nu\rangle^2 = (\nu_{\max} - \nu_{\min})^2/(\nu_{\max} + \nu_{\min})^2$. At later times, the viscosity distribution function is smoothed due to turbulent mixing and the temporal decay of the viscosity variance $\langle\nu'^2\rangle$.

3 Budget of the turbulent kinetic energy

An important question addressed by the present work is how the dissipation mechanism of turbulence is changed by variable viscosity, and whether turbulent flows with variable viscosity dissipate more or less energy as flows with constant viscosity. For decaying homogeneous isotropic turbulence the transport equation for the mean turbulent energy $\langle k\rangle = \langle u_i u_i\rangle/2$ reads

$$\frac{\mathrm{d}\langle k\rangle}{\mathrm{d}t} = \langle \frac{\partial \nu}{\partial x_i} \frac{\partial}{\partial x_j}\left(u_i u_j\right)\rangle - \langle\varepsilon\rangle_{\mathrm{VV}} . \qquad (7)$$

The first term on the right-hand side describes the dissipation of turbulent energy due to viscosity gradients. This term is negative, but DNS showed that it is negligible compared to the second term, which is the mean dissipation $\langle\varepsilon\rangle_{\mathrm{VV}} = \langle\nu\left(\partial u_i/\partial x_j\right)^2\rangle$ of turbulent energy. The mean dissipation is defined as the correlation between the local viscosity ν and the square of the local velocity gradient tensor

$$A_{ij} = \frac{\partial u_i}{\partial x_j} \,. \tag{8}$$

$\langle\varepsilon\rangle_{\mathrm{VV}}$ can be further decomposed by virtue of eq. (5) as

$$\langle\varepsilon\rangle_{\mathrm{VV}} = \underbrace{\langle\nu\rangle\langle\left(\frac{\partial u_i}{\partial u_j}\right)^2\rangle}_{\varepsilon_{CV}} + \underbrace{\langle\nu'\left(\frac{\partial u_i}{\partial u_j}\right)^2\rangle}_{\varepsilon_p} \,. \tag{9}$$

The first term on the right hand side of (9) denotes the classical dissipation for flows with constant viscosity, while the second term accounts for dissipation due to fluctuations of the viscosity. Figure 1 shows the temporal evolution of the terms appearing in (9) for the three cases under consideration. The mean dissipation $\langle\varepsilon\rangle_{\mathrm{VV}}$ displays an initial transient before turning into a decaying state, and is only slightly affected by the viscosity ratio R_ν. During the transient period the increase of $\langle\varepsilon\rangle_{\mathrm{VV}}$ is delayed for the two cases with variable viscosity. During the early phase of the decay, $\langle\varepsilon\rangle_{\mathrm{VV}}$ of the variable viscosity cases exceeds the constant viscosity case, indicating an enhanced turbulent mixing process. At later times, when turbulent mixing advances and the amplitude of viscosity fluctuations decreases, no difference between the different cases can be discerned. Figure 2 shows the temporal evolution of the turbulent energy $\langle k\rangle$. A slightly reduced initial decay of the turbulent energy is visible for the cases with variable viscosity, which is consistent with the temporal evolution of the dissipation $\langle\varepsilon\rangle_{\mathrm{VV}}$. These results confirm the trends previously reported by Taguelmimt *et al.* (2016*b*,*a*) in DNS studies of temporally evolving mixing layers.

In a next step, the effect of variable viscosity on the terms of eq. (9) is analyzed in more detail. Figure 1 shows that different from $\langle\varepsilon\rangle_{\mathrm{VV}}$, both $\langle\varepsilon\rangle_{\mathrm{CV}}$ and $\langle\varepsilon\rangle_{\mathrm{p}}$ strongly depend on the viscosity ratio R_ν. The dissipation $\langle\varepsilon\rangle_{\mathrm{CV}}$, which is built with the mean viscosity $\langle\nu\rangle$, is positive and increases with increasing viscosity ratio R_ν and clearly exceeds the mean dissipation $\langle\varepsilon\rangle_{\mathrm{VV}}$. As the mean viscosity $\langle\nu\rangle$ is the same for all cases, this indicates that turbulent flows with variable viscosity are characterized by larger velocity gradients $\langle A_{ij}^2\rangle$. In the balance of eq. (9) the strong dependence of $\langle\varepsilon\rangle_{\mathrm{CV}}$ on R_ν is compensated by the term $\langle\varepsilon\rangle_{\mathrm{p}}$ formed with the fluctuating part of the viscosity ν'. Initially $\langle\varepsilon\rangle_{\mathrm{p}}$ is zero because viscosity fluctuations and velocity gradients are uncorrelated. During the transient period $\langle\varepsilon\rangle_{\mathrm{p}}$ becomes negative and tends to zero again for larger times. Due to the balance between the positive $\langle\varepsilon\rangle_{\mathrm{CV}}$ and the negative $\langle\varepsilon\rangle_{\mathrm{p}}$, the mean dissipation $\langle\varepsilon\rangle_{\mathrm{VV}}$ is only slightly depending on R_ν.

Let us now analyze the link between ν and A_{ij}^2 by probability density functions (pdf). Both dissipation and velocity gradients are characterized by large fluctuations, which exceed the respective mean value by orders of magnitude. This phenomenon is known as internal intermittency. Figure 3 illustrates (for the time $t/\tau = 9.3$) the normalized pdfs of A_{ij}^2 and νA_{ij}^2 conditioned on $\phi \geq 0$ and $\phi < 0$, respectively (note that ν is linearly related to ϕ by eq. (5)). The pdf of A_{ij}^2 has stretched exponential tails, where the tail in the low viscosity regime is significantly pronounced compared to the high viscosity regime. These tails originate from strong rare events which are non-universal and generally depend on Reynolds number (or viscosity). As large velocity gradients occur at low viscosity (and vice versa), cf. fig. 4, the normalized conditional pdf of the dissipation reveals a notably reduced dependence on viscosity, which signifies that statistics of the dissipation $\langle\varepsilon\rangle_{\mathrm{VV}}$ become independent of viscosity. Note that a negative correlation between A_{ij}^2 and ν is a necessary condition for the independence of the dissipation from viscosity.

Statistics of the dissipation are now studied by the conditional average $\langle\varepsilon|\phi\rangle$, which provides further information about the correlation between dissipation

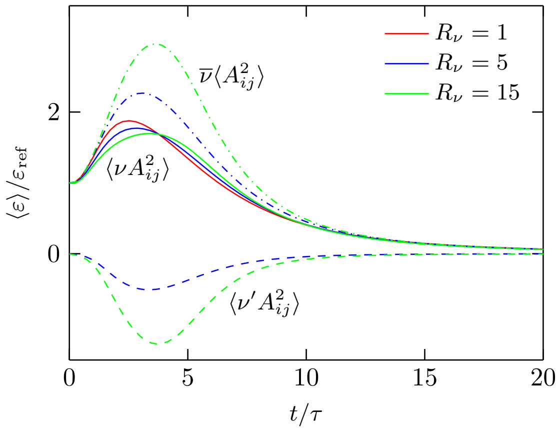

Figure 1. Temporal evolution of the terms appearing in eq. (9), i.e. the mean dissipation $\langle\varepsilon\rangle_{\mathrm{VV}} = \langle\nu A_{ij}^2\rangle$ (solid lines), the dissipation formed with the mean viscosity $\langle\varepsilon\rangle_{\mathrm{CV}} = \langle\nu\rangle\langle A_{ij}^2\rangle$ (dashed-dotted lines) and the fluctuating part $\langle\varepsilon\rangle_{\mathrm{p}} = \langle\nu' A_{ij}^2\rangle$ (dashed lines). The latter term is not shown for $R_\nu = 1$, as it is zero by definition. The time is normalized by $\tau = 1/(\kappa_p u_{\mathrm{rms,o}})$. The reference dissipation is chosen as $\varepsilon_{\mathrm{ref}} = \langle\varepsilon\rangle(t=0)$

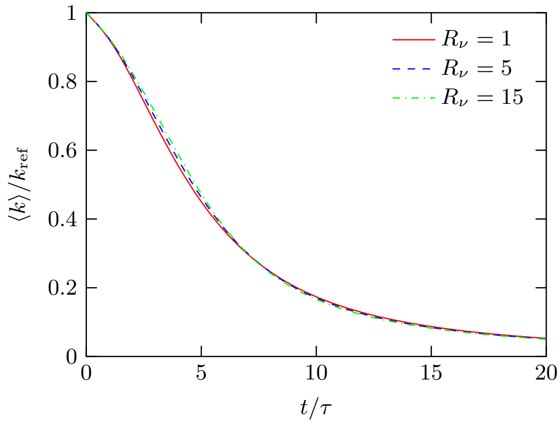

Figure 2. Temporal evolution of the mean turbulent kinetic energy $\langle k\rangle$ for the three viscosity ratios R_ν. The time is normalized by $\tau = 1/(\kappa_p u_{\mathrm{rms,0}})$, and $k_{\mathrm{ref}} = \langle k\rangle(t=0)$.

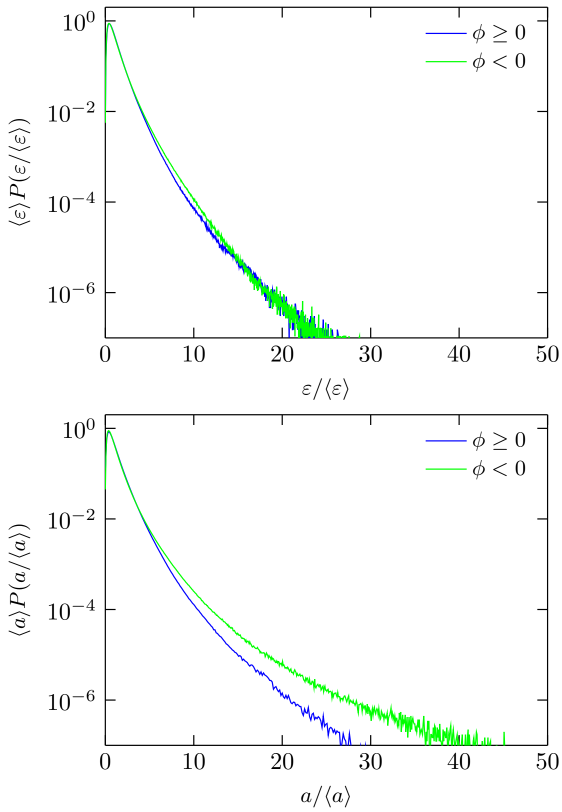

Figure 3. Normalized marginal pdf of $\varepsilon = \nu A_{ij}^2$ (top) and $a = A_{ij}^2$ (bottom), conditioned on positive and negative values of ϕ. Note that ν is linearly related to ϕ by eq. (5). The curves are normalized by the individual mean values $\langle\varepsilon\rangle$ and $\langle a\rangle = \langle A_{ij}^2\rangle$, respectively. The figure shows the case $R_\nu = 15$ at $t/\tau = 9.3$.

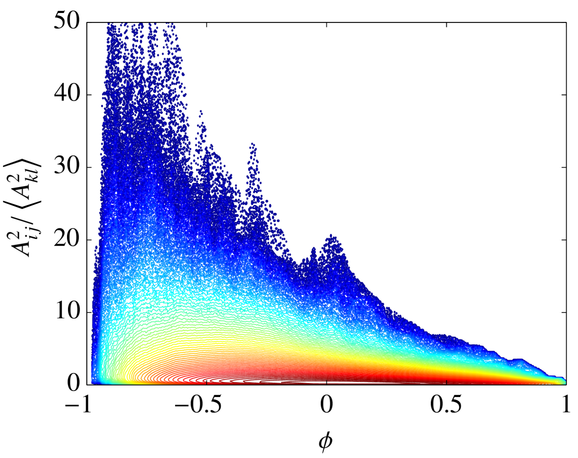

Figure 4. Joint pdf $P(A_{ij}^2, \phi)$ indicates the presence of large velocity gradients especially in the low viscosity regime for $\phi < 0$. The figure shows the case $R_\nu = 15$ at $t/\tau = 9.3$.

and viscosity. Figure 5 reveals that the conditional dissipation $\langle\varepsilon|\phi\rangle$ is asymmetric for $R_\nu > 1$, where during the early phase of transition ($t/\tau = 3.1$) large dissipation values occur on average for $\phi > 0$. At $t/\tau = 6.2$ the dissipation decays, but the decay rate is more rapidly in the high-viscosity region for $\phi > 0$

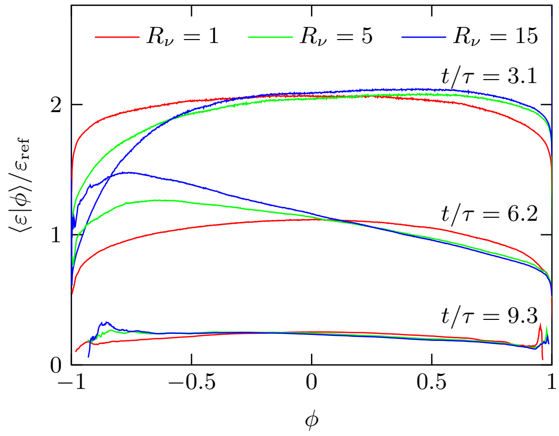

Figure 5. Mean dissipation $\langle\varepsilon|\phi\rangle$ conditioned on the scalar ϕ for three different times. The reference dissipation is defined as $\varepsilon_{\mathrm{ref}} = u_{\mathrm{rms},0}^3 \kappa_p$.

and, hence, the asymmetry is inverted and the highest dissipation level is observed in the low viscosity regime for $\phi < 0$. At later times ($t/\tau = 9.3$) the conditional dissipation $\langle\varepsilon|\phi\rangle$ decays further and becomes nearly independent of viscosity. Additionally, the value of $\langle\varepsilon|\phi\rangle$ is virtually independent of R_ν. These findings support the validity of Taylor's postulate for turbulent flows with variable viscosity.

4 Impact of viscosity fluctuations on the Kolmogorov length scale

Kolmogorov's theory postulates the existence of a dissipative cut-off scale where the turbulent cascade ends. This length scale is known as the Kolmogorov length scale η,

$$\eta = \left(\frac{\nu^3}{\varepsilon}\right)^{1/4}, \tag{10}$$

which is itself a fluctuating quantity. High values of the dissipation occur around thin sheet or tube-like regions with length scales smaller than the Kolmogorov length scale $\eta_0 = (\langle\nu\rangle^3/\langle\varepsilon\rangle)^{1/4}$ built with the mean values of the viscosity and the dissipation. The normalized probability density function (pdf) of the local Kolmogorov length scale is displayed in fig. 6 for all cases for $t/\tau = 6.2$. The left tail of the pdf, which is dominated by large intermittent fluctuations of the dissipation, reveals a strong dependence on the viscosity ratio R_ν. The cases with variable viscosity show a clear tendency to establish significantly smaller cut-off scales than the case with $R_\nu = 1$. On the other hand, the right tail of the pdf is nearly unaffected by viscosity fluctuations. These findings indicate that particularly the strong intermittent events of turbulence are enhanced by the fluctuations of viscosity, resulting in the presence of smaller length scales and a modified turbulent mixing. A further justification of these results is provided by the joint pdf of the velocity gradients and the viscosity $P(A_{ij}^2, \phi)$, where the largest velocity gradients A_{ij}^2 occur in the regime of low viscosity, see fig. 4. This signifies that the

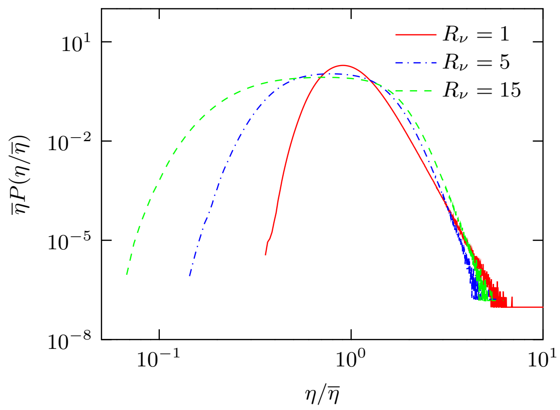

Figure 6. Normalized probability density function of the Kolmogorov length scale $\eta = (\nu^3/\varepsilon)^{1/4}$ at $t/\tau = 6.2$. The curves are normalized by $\overline{\eta} = (\langle\nu\rangle^3/\langle\varepsilon\rangle)^{1/4}$ from the constant viscosity case.

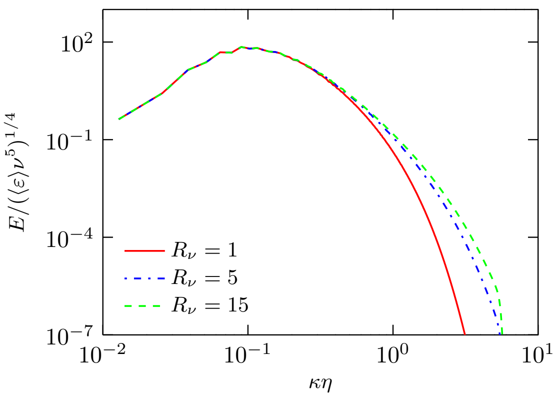

Figure 7. Normalized energy spectra $E(\kappa)$ for $t/\tau = 6.2$. For normalization the mean dissipation $\langle\varepsilon\rangle$ and Kolmogorov length scale for the constant viscosity case are used.

smallest length scales occur as expected in regions of low viscosity.

5 Two-point statistics

In the previous sections we have shown that fluctuations of the viscosity have a strong impact on the small scales of turbulence while statistics at the large scales are virtually unchanged. Energy spectra are considered to examine the scale-dependent effect of viscosity fluctuations on the turbulent cascade. Figure 7 shows the normalized energy spectra for all cases for $t/\tau = 6.2$. A difference between the constant and variable viscosity cases is clearly seen at the small scales, where the spectra for the variable viscosity cases extend towards large wave-numbers. This difference has a negligible effect on the mean turbulent energy but a considerable effect on the mean dissipation, cf. figs. 1 and 2. For later times, $t/\tau > 10$, the energy spectra for all cases collapse (not shown here) as the dissipation and the turbulent energy become independent of R_ν.

A central quantity of turbulence is the velocity increment $\Delta u = u(\boldsymbol{x}+\boldsymbol{r}) - u(\boldsymbol{x})$, defined at two points separated by a distance $\boldsymbol{r}$, whose moments are known as structure functions. Scale-dependent properties can be analyzed by structure functions, as they capture not only local but also non-local phenomena, which are inherent to turbulent flows. Kolmogorov's first similarity hypothesis states that for locally isotropic turbulence, statistics of velocity increments are determined uniquely by $\langle\nu\rangle$ and $\langle\varepsilon\rangle_{\mathrm{CV}}$. In other words, in the limit $r \to 0$, the second order structure function $\langle(\Delta u)^2\rangle$ can be developed in a Taylor series, i.e.

$$\langle(\Delta u)^2\rangle = \langle\left(\frac{\partial u}{\partial x}\right)^2\rangle r^2 = \frac{1}{15}\frac{\langle\varepsilon\rangle_{\mathrm{CV}}}{\langle\nu\rangle} r^2 \,, \tag{11}$$

and is uniquely determined by $\langle\nu\rangle$ and $\langle\varepsilon\rangle_{\mathrm{CV}}$. Equation (11) is an analytic solution of structure functions in the dissipative range. In the derivation of eq. (11) it is assumed without loss of generality that the separation vector $\boldsymbol{r}$ is aligned with the x axis. In the second equality the factor 1/15 is obtained by relating $\langle\varepsilon\rangle_{\mathrm{CV}}$ to $\langle(\partial u/\partial x)^2\rangle$ due to isotropy. In the large scale limit for $r \to \infty$, the second order structure function becomes independent of r and tends to its one-point limit, which equals $2\langle u^2\rangle$. Figure 8 shows the velocity structure function $\langle(\Delta u)^2\rangle$ for different times for the constant and variable viscosity cases under consideration. The structure functions are compensated by the dissipative range scaling yielding a plateau for $r \to 0$. A dependence of the structure function on the viscosity ratio is observed in the dissipative range for the time steps $t/\tau = 2.0$ and $t/\tau = 3.1$, which is in agreement with the dependence of $\langle A_{ij}^2\rangle$ on R_ν. At later times or at larger scales, $\langle(\Delta u)^2\rangle$ is independent of R_ν, which is in agreement with the independence of $\langle k\rangle$ on R_ν.

Now, we consider the viscosity-velocity structure function, defined as

$$S_\nu = \langle(\nu(\boldsymbol{x}+\boldsymbol{r}) + \nu(\boldsymbol{x}))(u(\boldsymbol{r}+\boldsymbol{r}) - u(\boldsymbol{x}))^2\rangle \,, \tag{12}$$

which appears in the diffusive term of the generalized transport equation for $\langle(\Delta u)^2\rangle$ in variable viscosity turbulence, cf. Voivenel *et al.* (2016) and Danaila *et al.* (2017). Equation (12) can be developed in a Taylor-series for $r \to 0$, yielding

$$S_\nu = 2\langle\nu\left(\frac{\partial u}{\partial x}\right)^2\rangle r^2 = \frac{2}{15}\langle\varepsilon\rangle_{\mathrm{VV}} r^2 \,, \tag{13}$$

where the second equality on the right-hand side exploits isotropy of the velocity field. In the large scale limit $r \to \infty$, S_ν becomes independent of r and tends to $4\langle\nu u^2\rangle$. Under the assumption that the viscosity is statistically independent from the turbulent energy, $4\langle\nu u^2\rangle$ simplifies to $4\langle\nu\rangle\langle u^2\rangle$. The viscosity-velocity structure functions are shown in fig. 8. Different to $\langle(\Delta u)^2\rangle$, the viscosity-velocity structure functions collapse for all time steps under consideration over all scales r independently of R_ν. This result has two implications. Firstly, at the small scales it confirms Taylor's postulate. Secondly, it underlines that large-scale statistics are not affected by fluctuations of the viscosity and confirms the independence between u^2 and ν.

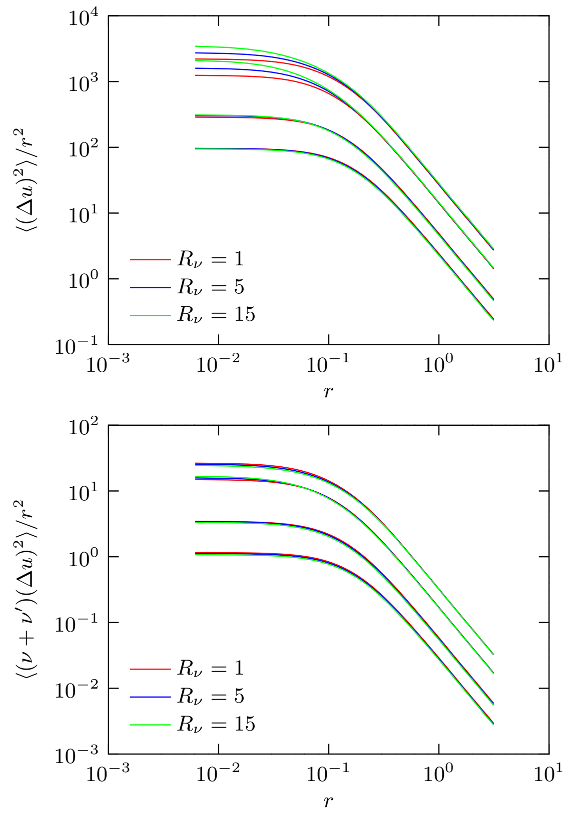

Figure 8. Compensated second order velocity structure function (top) and compensated mixed viscosity-velocity structure function (bottom) for different times t/τ (from top to bottom 2.0, 3.1, 6.2, 9.3) and viscosity ratios R_ν.

6 Conclusion and discussion

The present study focuses on the analysis of small-scale turbulence with variable viscosity by means of direct numerical simulations. The main results are:
(i) The effect of variable viscosity is virtually negligible on the mean turbulent energy $\langle k\rangle$ and the mean dissipation $\langle\varepsilon\rangle_{\mathrm{VV}}$. This finding confirms the validity of Taylor's postulate.
(ii) Turbulent flows with variable viscosity reveal significantly enhanced velocity gradients in regions of low viscosity, which results in the presence of smaller length scales and an increased level of small-scale intermittency.
(iii) It was shown that fluctuations of the viscosity affect the smallest scales of the flow but keep the larger scales unchanged.

Acknowledgment

Financial support was provided by the Labex EMC3, under the grant VAVIDEN, as well as the Normandy Region and FEDER. Additionally, the authors gratefully acknowledge the computing time granted on the supercomputer JUQUEEN (by the John von Neumann Institute for Computing), and the supercomputer TURING (by GENCI).

REFERENCES

Batchelor, GK & Townsend, AA 1949 The nature of turbulent motion at large wave-numbers. *Proceedings of the Royal Society of London. Series A. Mathematical and Physical Sciences* **199** (1057), 238–255.

Danaila, L, Voivenel, L & Varea, E 2017 Self-similarity criteria in anisotropic flows with viscosity stratification. *Physics of Fluids* **29** (2), 020716.

Gauding, M., Goebbert, J. H., Hasse, C. & Peters, N. 2015 Line segments in homogeneous scalar turbulence. *Physics of Fluids* **27** (9), 095102.

Gréa, Benoît-Joseph, Griffond, Jérôme & Burlot, Alan 2014 The effects of variable viscosity on the decay of homogeneous isotropic turbulence. *Physics of Fluids* **26** (3), 035104.

Ishida, T, Davidson, PA & Kaneda, Y 2006 On the decay of isotropic turbulence. *Journal of Fluid Mechanics* **564**, 455–475.

Kolmogorov, A. N. 1941*a* Dissipation of energy in locally isotropic turbulence. In *Dokl. Akad. Nauk SSSR*, , vol. 32, pp. 16–18. JSTOR.

Kolmogorov, A. N. 1941*b* The local structure of turbulence in incompressible viscous fluid for very large reynolds numbers. In *Dokl. Akad. Nauk SSSR*, , vol. 30, pp. 301–305. JSTOR.

Lele, S. K. 1992 Compact finite difference schemes with spectral-like resolution. *Journal of computational physics* **103** (1), 16–42.

Sreenivasan, KR & Antonia, RA 1997 The phenomenology of small-scale turbulence. *Annual review of fluid mechanics* **29** (1), 435–472.

Taguelmimt, N., Danaila, L. & Hadjadj, A. 2016*a* Effect of viscosity gradients on mean velocity profile in temporal mixing layer. *Journal of Turbulence* **17** (5), 491–517.

Taguelmimt, N., Danaila, L. & Hadjadj, A. 2016*b* Effects of viscosity variations in temporal mixing layer. *Flow, Turbulence and Combustion* **96** (1), 163–181.

Talbot, B, Danaila, L & Renou, B 2013 Variable-viscosity mixing in the very near field of a round jet. *Physica Scripta* **2013** (T155), 014006.

Talbot, Benoît, Mazellier, Nicolas, Renou, Bruno, Danaila, Luminita & Boukhalfa, Mourad Abdelkrim 2009 Time-resolved velocity and concentration measurements in variable-viscosity turbulent jet flow. *Experiments in fluids* **47** (4-5), 769–787.

Taylor, Geoffrey Ingram 1935 Statistical theory of turbulence. In *Proceedings of the Royal Society of London A: Mathematical, Physical and Engineering Sciences*, , vol. 151, pp. 421–444. The Royal Society.

Voivenel, L, Danaila, L, Varea, E, Renou, B & Cazalens, M 2016 On the similarity of variable viscosity flows. *Physica Scripta* **91** (8), 084007.

Warhaft, Z. 2000 Passive scalars in turbulent flows. *Annual Review of Fluid Mechanics* **32** (1), 203–240.